Egyptian Geophysical Society
EGS Journal, Vol. 13, No. 1, 45-56 (2015)

RECOGNITION OF MEGA STRUCTURES OF SINAI PENINSULA USING POTENTIAL FIELD DATA

K.S. Essa[(1)], A.G. Nady[(2)] and M. Elhussein[(1)]

(1) Geophysics department, Faculty of Science, Cairo University, Egypt.
(2) Nuclear Materials Authority, P.O. Box 530 Maadi, Cairo, Egypt.

التعرف على التراكيب الضخمة فى شبه جزيرة سيناء باستخدام معطيات البيانات المغناطيسية

الخلاصة: الهدف من هذه الدراسة هو شرح العناصر الهيكلية الضخمة وتحديد إطار التكتونية لشبه جزيرة سيناء، مصر. وقد تم تنفيذ هذه الدراسة من خلال الطريقة المغناطيسية، وسيتم تحليل البيانات المغناطيسية لتحديد العمق إلى سطح صخور القاع من طرق مختلفة، على سبيل المثال، طريقة ايولر، سيتم استخدام الأعماق الناتجة من البيانات المغناطيسية بمثابة نقاط مراقبة في بنلء نماذج ثنائية ونصف الأبعاد من أجل تقليل الخطأ وتسهيل التكرار من النماذج المقترحة، هذه النماذج المختلفة تشير إلى زيادة العمق الى سطح صخور القاع من الجنوب إلى شمال سيناء، هذا العمق لسطح صخور القاع يتراوح من ظهور على السطح في جنوب سيناء إلى أكثر من ٤ كم فى شمال سيناء.

ABSTRACT: *The objective of this study is to explain the mega structural elements and to determine the tectonic framework of Sinai Peninsula, Egypt. This study has been implemented by the magnetic method. Magnetic data will be analyzed to determine the depth to the basement surface by using Euler deconvolution method and power spectrum. The depths obtained from magnetic data will be used as a control point in the 2.5D magnetic modelling in order to minimize the error and facilitate the iteration of the suggested models. These different models indicate that the depth to basement surface increases from South to Northern Sinai. This depth to basement surface ranges from basement outcrop in southern Sinai to more than 4km in northern Sinai.*

1. INTRODUCTION

Sinai Peninsula is a triangular wedge which lies between latitudes 27°44' and 31°20' North and longitudes 32°18' and 34°54' East, It occupies an area of almost 61,000 km^2 and separated geographically from Africa by the Suez Canal and the Gulf of Suez rift. It is bounded by the Mediterranean Sea to the north, the Gulf of Suez to the west, and the Gulf of Aqaba to the east. (Fig. 1)

The objective of this study is to delineate the impact of different structures in Sinai Peninsula on the magnetic data. This is done by using the following steps:

1) Regional-Residual separation was carried out using power spectrum in Geosoft software for magnetic data.
2) Depth to the basement surface was estimated using Euler deconvolution and power spectrum.
3) A magnetic modelling was applied along two selected profiles to determine the basement configuration in the Sinai area. In these models the calculated anomalies fit with the observed one.

2. GEOLOGIC SETTING OF SINAI PENINSULA

Sinai Peninsula is wedged between Africa, Anatolian, and Arabian plates, constituting a transition between the Eastern Egyptian desert and the Middle East region (Ben-Menahem et al., 1976; McKenzie et al., 1970). These regional/plates have been shaped since the Early Mesozoic by a series of rifting phases that formed the northeastern margin of the Afro-Arabian continent (Ben-Avraham and Ginzburg, 1990; Garfunkel, 1998). The boundaries of Sinai Peninsula are defined by the Gulf of Suez and the Gulf of Aqaba-Dead Sea fault System (Mckenzie et al., 1970).

In the south, the exposed Pre-Cambrian igneous and metamorphic rocks form the Arabo-Nubian shield which is a stable tectonic unit.

The central part of Sinai Peninsula consists of sub horizontal Mesozoic and Tertiary sediments, creating the plateau of Gebel El Tih-Egma that represents a thin sedimentary cover, which is affected only by normal faulting. These faults are of N–S to NNE–SSW, NW–SE and E–W trends (Fig. 2).

The Sinai Peninsula is bounded by major tectonic elements. These are the Mesozoic-Early Cenozoic tectonically-active Tethys Sea to the north, the Oligo-Miocene Gulf of Suez rifted basin to the west, and the late Miocene to Recent transform Dead Sea-Gulf of Aqaba rift to the east.

Stratigraphy:

Paleozoic Sequence:

The Paleozoic sediments are exposed only in south central parts of Sinai Mostly in the Um Bogma area east of Abu Zenima and at Abu Durba area. The lithostratigraphic section of Paleozoic sequence is illustrated in Figure3. The thickness of the Paleozoic section increases northwards and where there is a greater marine facies influence.

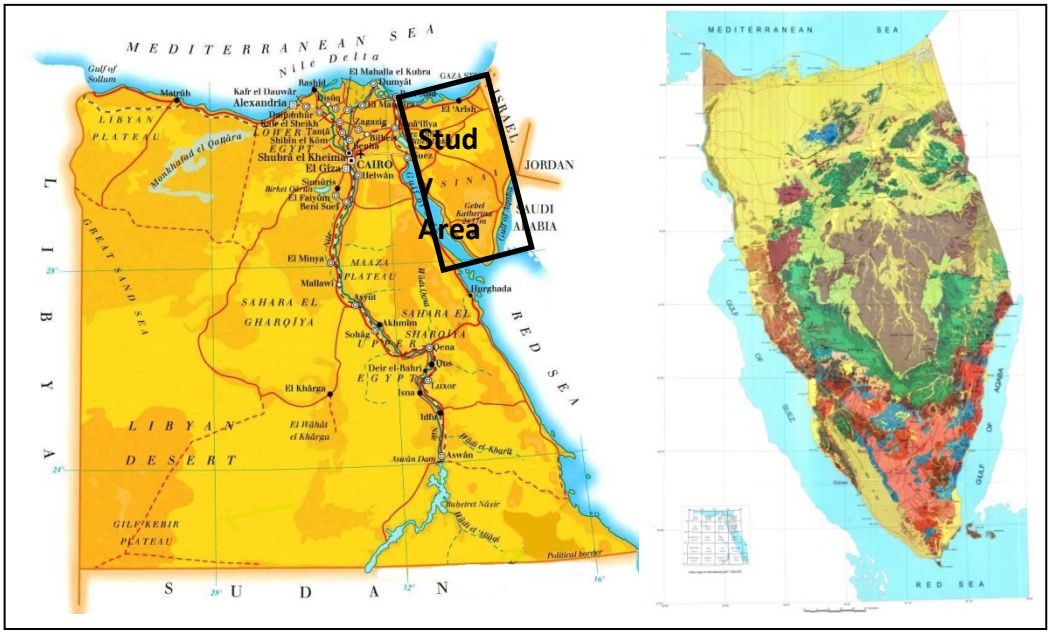

Fig. (1): Location map of the study area.

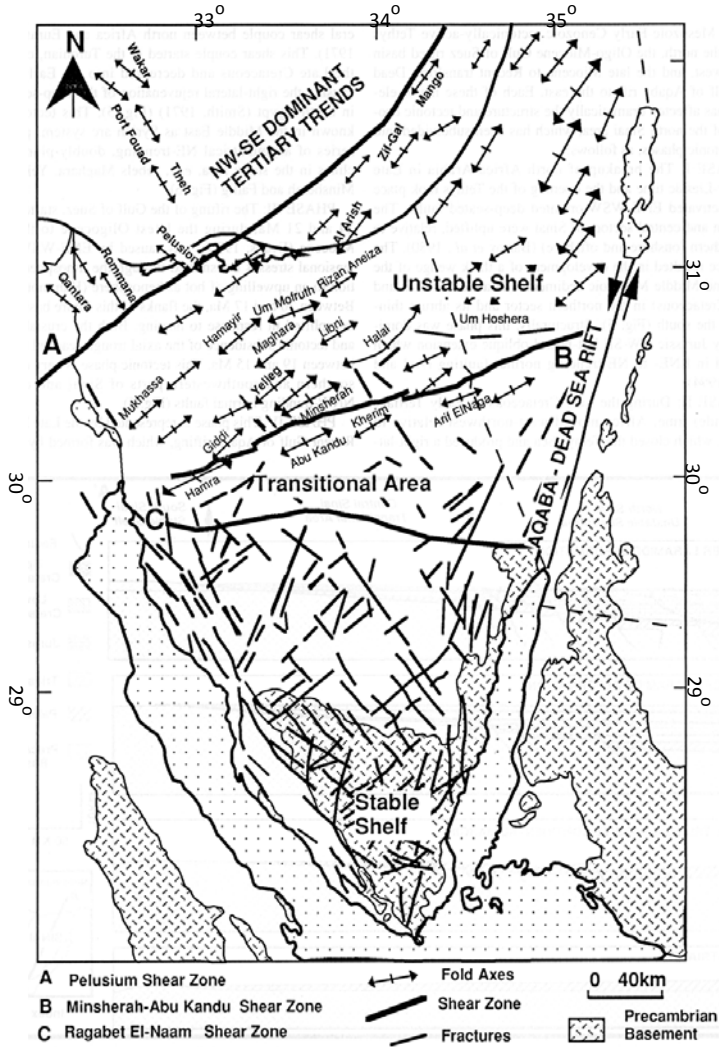

Fig. (2): Major tectonic elements in Sinai Peninsula,Egypt. (After Neev, 1975).

This succession is subdivided into the following formations: The Basal Cambro-Ordivician sequence represented by Araba, Naqus and Wadi Malk Formations of Issawi and Jux (1982); These clastic sediments are dominated by grits, siltstones, subarkoses ,and conglomerates,with a few dolomite beds. These sediments were deposited under fluvial-paralic conditions; The Lower Carboniferous Um Bogma Formation represents the first reliable date for Paleozoic sequence in Sinai; These marine carbonates are richly fosilliferous especially Foraminifera and have been dated as Tournaisian-Visean; Ataqa Formation (Upper Carboniferous), which is characterized by thick cross-bedded, very fine to fine grained sandstones unconformably overlying the Um Bogma Formation.

In central and south Sinai, the Permian is represented by the continental sediments of the Budra or Qiseib Formation. In north Sinai there is neither surface nor subsurface data available on the Permian, although it is highly probable that marine conditions existed in this area during this period.

Mesozoic Sequence:

Triasic:

In Sinai, the only outcrop of Triassic sediments is in the core of Gebel Arif El Naga (Awad, 1946; Karcz and Zak, 1968), while in the subsurface they have only penetrated in the Halal-1 borehole where the Triassic thickness was 914m.

The Triassic sediments are represented in Arif El Naga Formation, which consist of continental clastics and marine limestones exposed in Jebel Arif El Naga.

Jurassic:

The most complete Jurassic sequence (more than 1980m) is exposed in north Sinai at Gebel Maghara which is a large breached anticline with a gentle north flank and a steep, often vertical to overturned, southern flank.

Jurassic sediments are also exposed at Gebel Arif El Naga (141m), and Gebel Minshera(80m). The Jurassic facies in Sinai range from deep marine to shallow- marginal marine to continental-fluvial clastic sediments.

The Jurassic sequence is subdivided into the following formations: Mashabba Formation, which represents the lowermost Jurassic sequence, and characterized by clastic sediments of Liasic age, Bir Maghara Formation, and Safa Formation, which represents the middle Jurrasic sequence, and characterized by clastic carbonate sediments. This clastic-carbonate sequence is also exposed at Gebel Minsherah and has been penetrated in the Halal-1(780m) and Giddi-1(more than 805m) wells. Finally, Masajid Formation, which represents the upper Jurassic sediments, and dominated by carbonates representing a southerly marine transgression at the end of Bathonian-Callovian times.

Cretaceous:

Lower Cretaceous:

In central Sinai, the Pre-Cenomanian section is composed entirely of 'Nubian-type' sandstones which attain a thickness of 780m at Um-Bogma. The basal part (282m) of these sands have been assigned a Carboniferous age, whilst the upper 498m is thought to range from Triassic to Lower Cretaceous in age. These sandstones are exposed along the scarp of Gebel Tih.

'Nubian Type' sandstones of Early Cretaceous age have also been penetrated in the following boreholes; Abu Hamth (370m), Nekhl (247m), Ayum Musa-2 (149m), Hamra (366m) and Kabrit (103m).

Upper Cretaceous to late Eocene Sequence:

This sequence is characterized by the predominance of carbonates in the lithostratigraphic units; it is present on the surface and the subsurface of north Sinai and consists of two groups, in ascending order: Nezzazat (Cenomanian to Santonian) with thicknesses of 732, 845 and945 m in the Jebels Maghara, Arif Al Naqa and Minsherah, respectively, and El Egma (Campanian to Middle Eocene) (Fig. 3).

Cenozoic Sequence:

Oligocene:

The distribution of the Oligocene sediments, is known only from boreholes drilled in the extreme north of Sinai and in the offshore area.

The Oligocene sediments, known as Tayiba Red Beds (Barakat et al., 1988), are absent in the southern part of the onshore area due to the emergence of this sector as a result of the influence of the early stages of the Gulf of Suez rifting.

The thickness of the Oligocene sequence ranges from less than 152m in the northern most Sinai to more than 1800m in the offshore region.

Miocene:

The Miocene section ranges in thickness from 152m in onshore north Sinai to more than 1000m in the extreme north and offshore areas.

The Miocene section is subdivided into two formations, in ascending order:

Sidi Salem Formation (Lower to Middle Miocene) and Qawasim/Rosetta Formation (Middle to Upper Miocene) (Fig. 3).

Post-Miocene Sequence:

The thickness of the post-Miocene sequence is 400, 250, 1250 and 1700 m in wells Gal-1, Sneh-1, Qantara-1 and El Temsah-1, respectively.

The post-Miocene section is thin in wells located on old structural highs, e.g., Malha-1, where it has a thickness of only 88 m.

The Plio-Quaternary sequence is represented onshore by thin continental to littoral sediments which are approximately 3000m thick. See Figure 3.

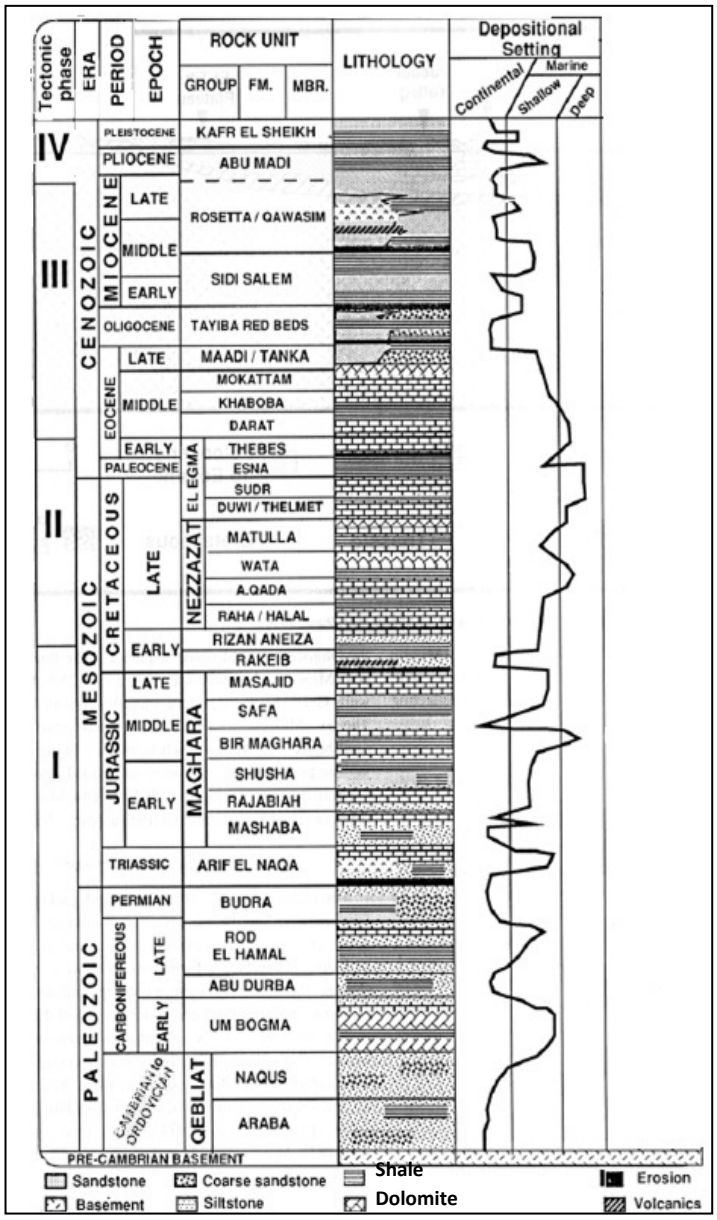

Fig. (3): Generalized stratigraphic column, depositional environments of Sinai Peninsula, Egypt.

The post-Miocene section is subdivided into the following formations, in ascending order: Abu Madi Formation (Pliocene) and Kafr El Sheikh (Pleistocene) (Said, 1962). (Fig. 3).

3. DATA AND METHODS

Magnetic measurements contain contributions from sources of interest at shallow depths (residual component) as well as contributions from sources at greater depths (regional component); Anomalies deduced from magnetic methods can be used to define and estimate the physical properties of the source structures that cause them.

Magnetic data for the entire Sinai Peninsula of about 3117 stations were measured with spacing 5km apart. The measured data was corrected to base station of continuous recording to check earth's Magnetic Field variation.

The measured data was tied to single base station at Abu Zeneima with Latitude 29°04'N and Longitude 33°11'E. The corrected data were edited, gridded, filtered and contoured with 5 gamma contour interval. This study was carried out as a part of the UNDP/UNSCO program (Ismail et al, 2001).

These measured data were then separated into regional and residual components using Geosoft software version 2007.

4. QUALITATIVE INTERPRETATION

4.1 Total magnetic intensity map:

The interpretation will depend on the total intensity magnetic map since the R.T.P(reduction to

pole) map is hard to produce as the shape of the surveyed area is irregular and as RTP filter is applied in Fourier domain; so the extension of the data at the edges of the map is not the same. Also the limitation of the RTP filter is that it can introduce noise into the resultant grid where the grid contains high frequency and high amplitude anomalies.

The Sinai peninsula is divided into two zones: The northern Sinai (Zone I) and the southern Sinai (Zone II).

These two zones are separated by the themed fault trending E-W (Fig. 4).

The first zone is characterized by gentle gradient and long wavelength which indicate the deeper basement surface in this zone.

From the total magnetic intensity map there are different ranges of magnetic amplitude. The first zone is characterized by three magnetic anomalies the first one ranges from 42298-42450 nT, taking red color (Fig. 4).This anomaly is present in very small areas in northern sector. The second magnetic anomaly range from 42208-42298nT, taking green color (Fig. 4) which is present in most areas of zone I. The third magnetic anomaly range from 42003-42208nT, which is lowest magnetic anomaly, This anomaly is present in different parts of the zone I as the depth to basement surface increase toward northern Sinai.

Zone II is characterized by two groups of different magnetic characters: The first group is characterized by green color which occupies small parts of zone II. Meanwhile the second group is characterized by two different types of magnetic anomalies of pink and red colors which constitute most of zone II area where the basement surface is shallow.

4.2 Regional magnetic map:

The interpretation of the regional magnetic map of Sinai Peninsula shows the general distribution of the magnetic anomaly patterns according to their shape and amplitude as well as the trends of the magnetic anomalies.

- From the regional magnetic map (Fig. 5), the first zone (zone I) is dominated by two low magnetic anomalies the first one ranges in value from 42290 to 42210nT, taking green color and no.3, trending NW-SE and N-S, the second anomaly is the lowest magnetic anomaly ranging from 42210-42145nT, marked by blue color, and no.4, trending N-S and E-W.
- There is also another magnetic anomaly in northern Sinai range from 42290 to 42450nT, marked by red color and no.2, trending NW-SE. This anomaly is located in small parts of zone I.
- The second zone(zone II) is dominated by two high magnetic anomalies; the first one ranges from 42290 to 42450nT, This anomaly is present in different parts of Zone II marked by red color and no.2 (Fig.5), trending E-W and NNE-SSW, while the second one is the highest magnetic anomaly and ranges from 42450 to 42660nT, marked by pink color and no.1(Fig.5), trending E-W, NNE-SSW and NNW-SSE.
- Another magnetic anomaly present in southern Sinai ranges from 42290-42210nT, marked by green color and no.3 (Fig.5). This anomaly is present only in one location in zone II, trending NE-SW.

The regional magnetic map may reflect the different composition of basement rocks.

4.3 Residual magnetic map:

The residual magnetic map shows the high frequency anomalies that are masked in regional magnetic map.

From the residual magnetic map (Fig. 6) the northern zone (zone I) is characterized by NE-SW, E-W, and NW-SE trending anomalies. The NE-SW trend is more dominant than NW-SE trend in northern zone. The presence of E-W trending anomalies in central Sinai zone is associated with the central Sinai shear zone.

While the southern zone (zone II) is characterized by NW trending anomalies along Gulf of Suez, NNE anomalies along Gulf of Aqaba and NE trending anomalies.

5. DEPTH DETERMINATION

5.1 Power spectrum technique:

A typical energy spectrum for magnetic data may exhibit three parts of the spectrum; a deep source component (regional) which is in low frequency end and in most cases is easier to approximate with a straight line denoting deeper discontinuities (Moho and/or Conrad), a shallow source component (residual) which is in high frequency end, with an undulating character, denoting shallower sources (basement and/or intrusions), and a noise component.

The depth (h) of an 'ensemble' of sources is easily determined by measuring the slope of the energy (power) spectrum (S) and dividing by 4 π (equation 1)

$$h = -S/4\pi \quad (1)$$

Figures 7 illustrates the interpretation of energy spectrum of magnetic data respectively into the three components by using Geosoft software. The ensemble magnetic depth estimates are based on 3 and 5 point averages of the slope of the energy spectrum (Spector and Grant, 1970).

From figure 7 the average depth of the regional component is about 5.6km while that of residual component is about 2km.

5.2 Euler deconvolution:

Euler deconvolution belongs to a class of techniques which are sometimes referred to as "automatic depth estimate methods".

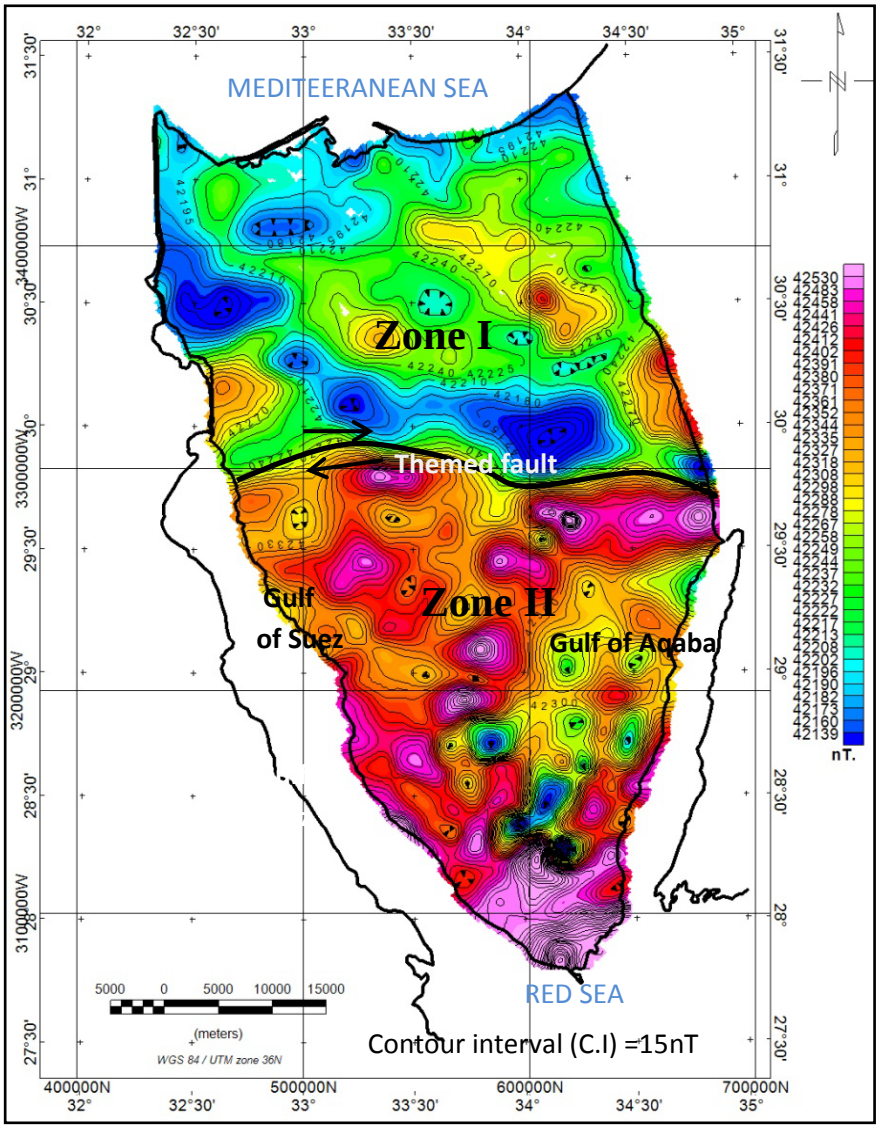

Fig. (4): Filled color contour map of Total magnetic intensity of Sinai Peninsula, Egypt.

The 3D form of Euler's equation can be defined by (Reid et al., 1990) as:

$$x\frac{\partial T}{\partial x}+y\frac{\partial T}{\partial y}+z\frac{\partial T}{\partial z}+\eta T=$$
$$x_o\frac{\partial T}{\partial x}+y_o\frac{\partial T}{\partial y}+z_o\frac{\partial T}{\partial z}+\eta b \quad (2)$$

Where x, y and z are the coordinates of a measuring point, x_o, y_o, and z_o are the coordinates of the source location, b is a base level, and η is a structural index defining the anomaly attenuation rate at the observation location, the following table (1) shows the different values of structural index for magnetic field.

Table (1): The structural index (S.I) of magnetic field.

S.I	Magnetic field
0	Contact / step
1	Sill/ Dyke
2	Cylinder/ pipe
3	Sphere/ Barrel/ordnance

The Euler deconvolution method is done by Geosoft software version 6.4.2 on the magnetic data. The depths is divided into four levels the first one from depth 0km to1.5km the second level from 1.5 to3km, the third one from 3km to 4.5km and the fourth from 4.5 to 6km.

The Euler map of the magnetic data is shown in Figure 8 where the structural index is zero which indicates the location of contacts.

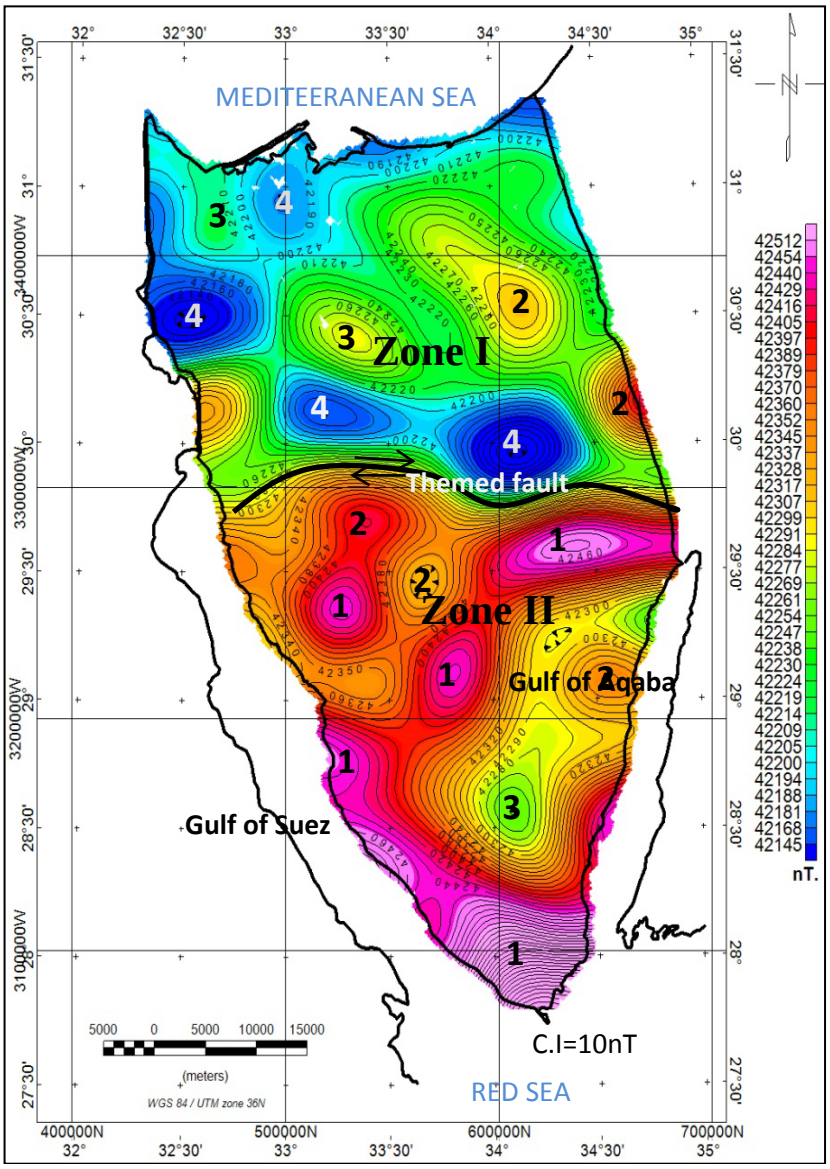

Fig. (5): Filled color contour map of Regional magnetic of Sinai Peninsula, Egypt.

6. MAGNETIC MODELLING

To confirm the interpreted magnetic basement structural framework of the study area, two regional magnetic profiles have been modeled using the 2.5 Dimensional modeling techniques by GM-SYS package in GEOSOFT software version 6.4.2 (2007). The selected profiles are taken from the regional magnetic map (Fig.10). The selection of the location of these profiles to delineate the Syrian Arc structures, the Sinai Hinge Belt and the Themed fault (Fig. 12).

This type of modeling is a reverse model that depends on the changes in the magnetic susceptibility, and the depth parameters till complete matching between the calculated and observed profiles. Magnetic susceptibility values for the different polygons were changed and readjusted during modelling. The resulting parameters represent the main target of this method (e.g., depth, magnetic susceptibility).

Profile A-A':

Figure10 shows a best fit between the observed regional magnetic profile and the computed magnetic field.

The regional basement configuration along this profile is shown on the lower half of figure 10. This regional basement configuration is composed of fourteen polygons of different magnetic susceptibilities ranging in value from 450 to 4800X10^{-6} c.g.s unit.

From Figure 10 it's shown that the depth to the basement top from the Abu Hamth well is matched with the model which is equal to 2.13km.

Profile B-B':

Figure 11 shows a best fit between the observed regional magnetic profile and the computed magnetic field.

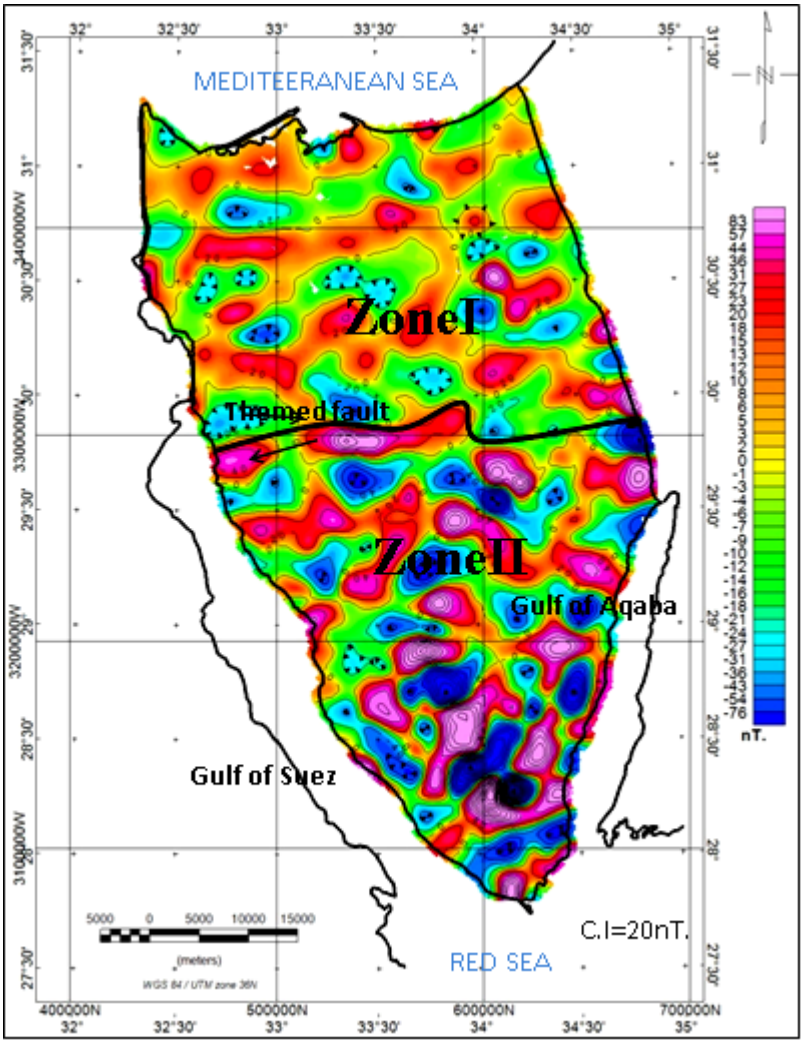

Fig. (6): Filled color contour map of Residual magnetic of Sinai Peninsula, Egypt.

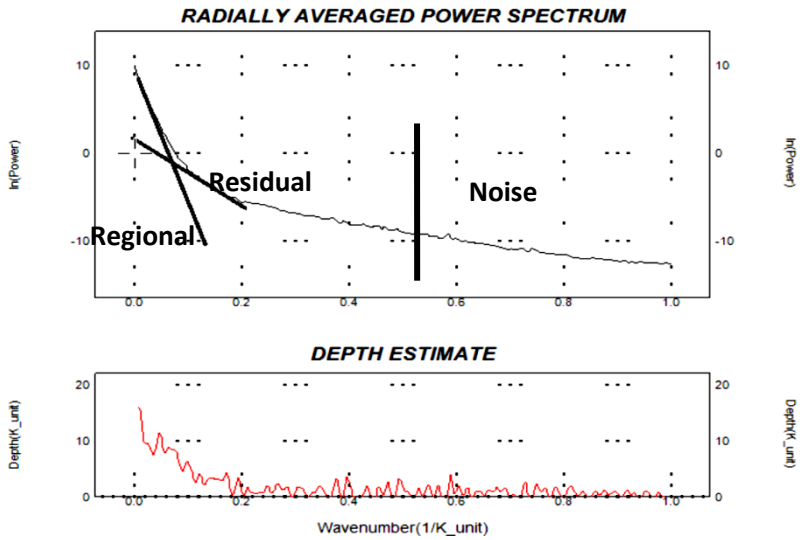

Fig. (7): Interpretation of the radially averaged energy (power) spectrum for magnetic data showing the three components.

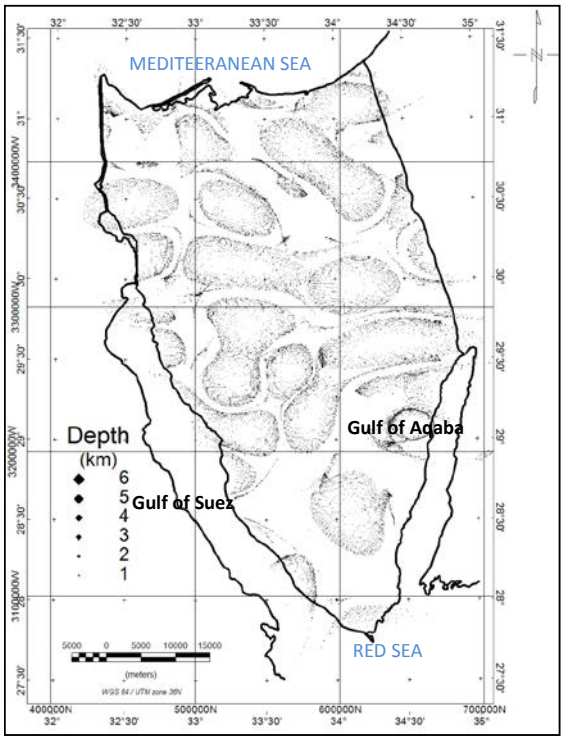

Fig. (8): Euler magnetic map for contacts (S.I=0).

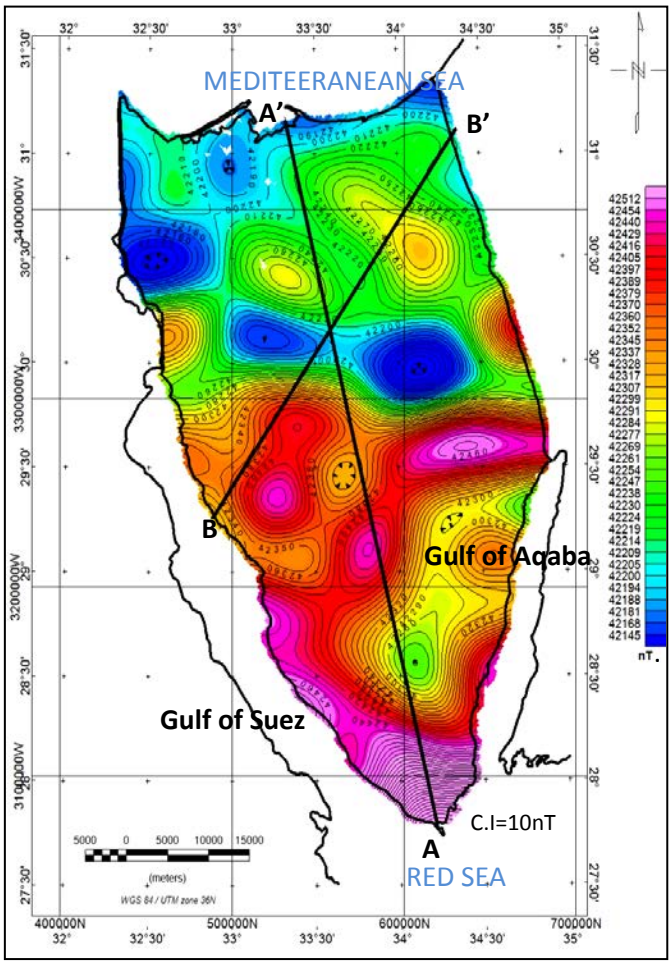

Fig. (9): Location of profiles taken along the study area.

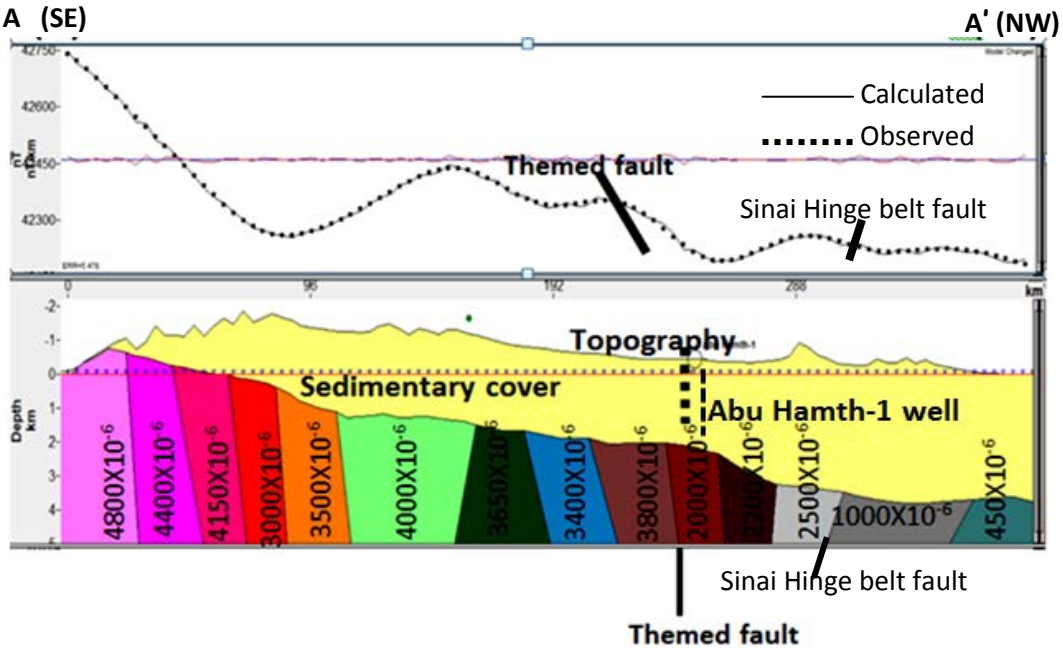

Fig. (10): The 2.5D magnetic model for profile A-A'.

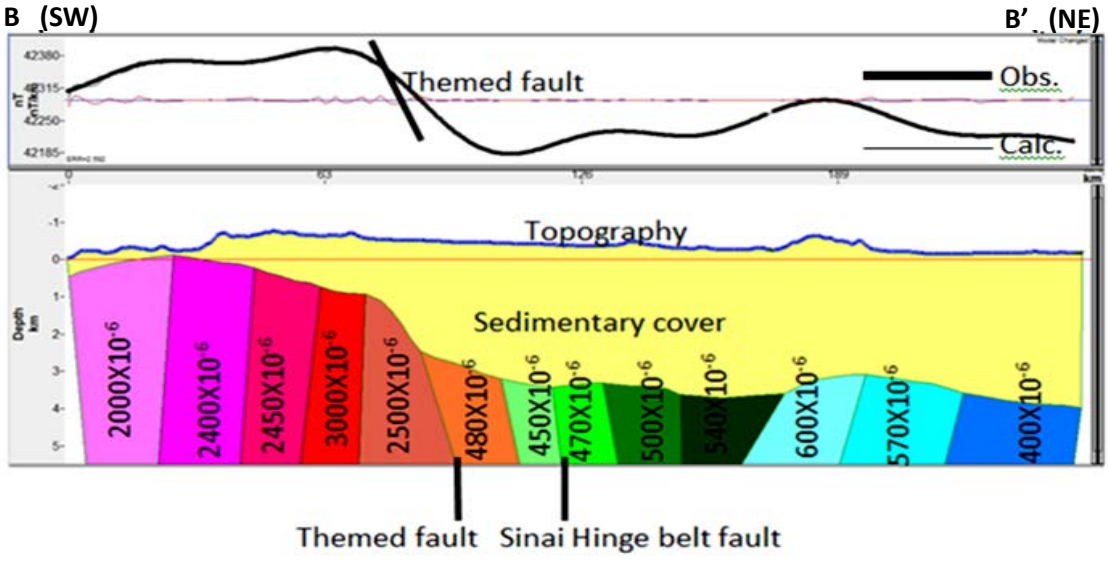

Fig. (11): The 2.5D magnetic model for profile B-B'.

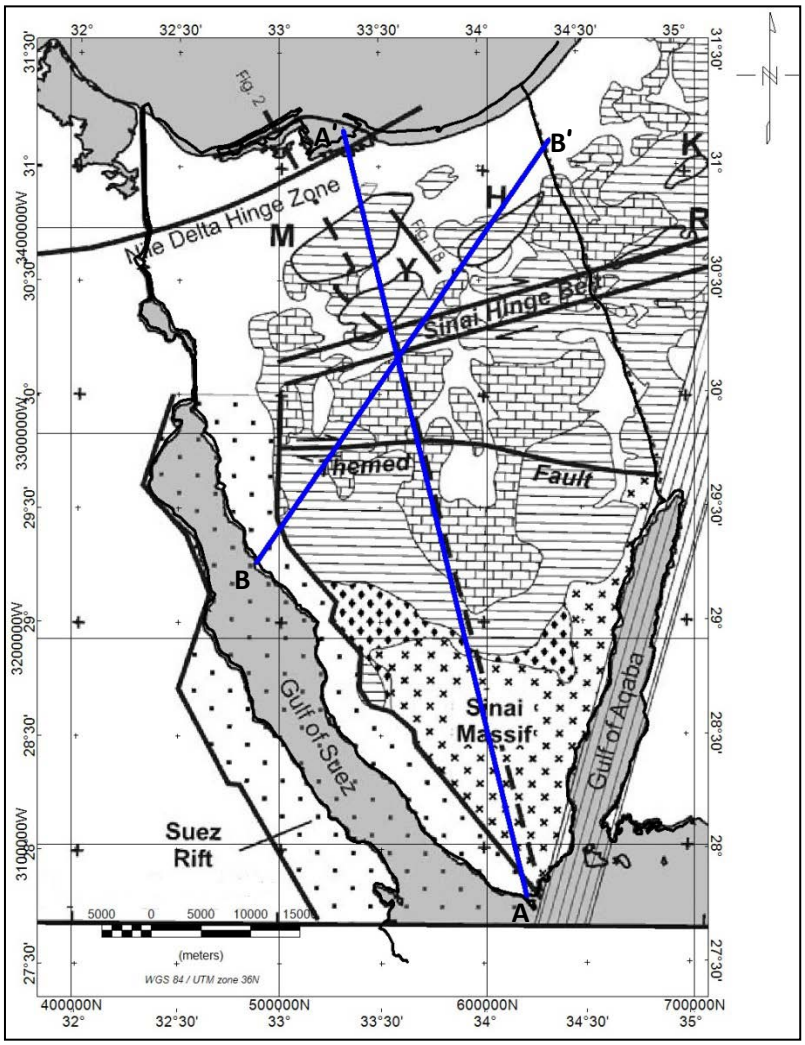

Fig. (12): The location of Sinai Hinge belt and the themed fault.

The regional basement configuration along this profile is shown on the lower half of Figure 12. This regional basement configuration is composed of thirteen polygons of different magnetic susceptibilities ranging in value from 400 to 3000x10^{-6}c.g.s unit.

7. CONCLUSIONS

- The depth to the basement is shallow in southern Sinai peninsula and becomes deep as we move toward north due to the basement outcrop in south Sinai. This gives high amplitude magnetic anomalies in southern Sinai than that in north.
- The magnetic susceptibilities in the area ranges from 400X10^{-6} to 4800X10^{-6} c.g.s. units which indicate the granitic and granitoiditic composition of the basement rocks.
- There are four major trends in the study area: NE (Syrian arc), NW (Gulf of Suez), E-W (Tethyan) and NNE (Aqaba) trend. The NE (Syrian arc) trend is more dominant in northern Sinai than that in southern Sinai while the NW (Gulf of Suez) trend is more dominant in the southern Sinai than that in northern Sinai.
- Two profiles pass through the Themed fault which is a very long east-west oriented fault zone that cuts the tectonically stable area lying south of the Sinai hinge belt (Fig.12). This fault zone extends for about 200 km from the vicinity of the eastern margin of the Suez rift to the Dead Sea transform. This fault was rejuvenated along a pre-existing fault marking the southernmost edge of the Early Mesozoic continental margin of the Eastern Mediterranean basin in central Sinai (Moustafa & Khalil, 1994).

The two profiles A-A', and B-B', pass through the Sinai hinge belt which is a narrow ENE–WSW oriented structural belt forming the boundary between the North Sinai folds and the platform area lying to the south. This belt is 15–20 km wide and is dominated by long segments of ENE– WSW oriented faults that show evidence of right lateral strike–slip displacement. These faults are shown in the A-A' models as they have ENE-WSW trend in the northern part of the model (Fig.10) and it is shown in the B-B' model in Figure 11.

REFERENCES

(Easternmost Mediterranean). Geology, v. 3, p. 683-686.

Awad, G.H. 1946. On the occurrence of marine Triassic (Muscchelkalk) deposits in Sinai. Bull. Inst. Egypt 27: 397-429.

Barakat, M.G., Darwish, M. and EI-Outefi; N.S. 1988. Eocene tectono-stratigraphy and basin evaluation in the Gulf of Suez petroliferous province. 9th EGPC Exploration Seminar, Egypt, v. I, 22p.

Ben-Avraham, Z., Ginzburg, A., 1990. Displaced terranes and crustal evolution of the Levant and East Mediterranean. Tectonics 9, 613–622.

Ben-Menahem, A., Amos, N., Moshe, V., 1976. Tectonics, seismicity and structure of the Afro-Eurasian Junction. The breaking of an incoherent plate. Phys. Earth Planet. Inter. 12 (1), 1–50.

Garfunkel, Z., 1998. Constraints on the origin and history of the Eastern Mediterranean basin. Tectonophysics 298, 5–35.

Ismail A.M., Sultan S.A. and Mohamady M.M., 2001. Complete Bouguer and total magnetic intensity of Sinai Scale 1:500.000, Abstracts, the 6th Conference "Geology of Sinai for Development", Ismailia.

Issawi, B. and Jux, U., 1982. Contributions to the stratigraphy of the Paleozoic rocks in Egypt.Geol.Surv.Egypt, paper 64,28pp

Karcz,I. and Zak, I., 1968. Paleocurrents in the Triassic sandstone of Arayif-En-Naga,Sinai.Isr. J. Earth Sci.17: 9-15.

McKenzie, D.P., Davies, D., Molnar, P., 1970. Plate tectonics of the Red Sea and East Africa. Nature 226, 243–248.

Moustafa, A.R. and Khalil, M.H., 1994. Rejuvenation of the Eastern Mediterranean passive continental margin in northern and central Sinai: new data from the Themed Fault. Geological Magazine, 131, 435–448.

Neev, D., 1975. Tectonic evolution of the Middle East and Lavantine basin

Reid, A.B., Allsop, J.M., Granser, H., Millett, A.J., Somerton, I.W., 1990. Magnetic interpretation in three dimensions using Euler deconvolution. Geophysics 55, 80–9.

Said, R., 1962. The Geology of Egypt.El sevier,377PP.

Spector, A. and Grant, F.S., 1970. Statistical models for interpreting aeromagnetic data. Geophysics 35, 293–302.